

## **An ultrafine iridium nanoparticle prepared without surfactant for acidic oxygen evolution reaction**

Anyang Chen,<sup>1#</sup> Mengting Deng,<sup>1#</sup> Zhiyi Lu,<sup>1,2</sup> Yichao Lin,<sup>1,2\*</sup> Liang Chen,<sup>1,2\*</sup>

[1] Key Laboratory of Advanced Fuel Cells and Electrolyzers Technology of Zhejiang Province, Ningbo Institute of Materials Technology and Engineering, Chinese Academy of Sciences, Ningbo, Zhejiang 315201, P.R. China

[2] University of Chinese Academy of Sciences, Beijing 100049, P.R. China

# These authors contribute equally

E-mail: [yclin@nimte.ac.cn](mailto:yclin@nimte.ac.cn), [chenliang@nimte.ac.cn](mailto:chenliang@nimte.ac.cn)

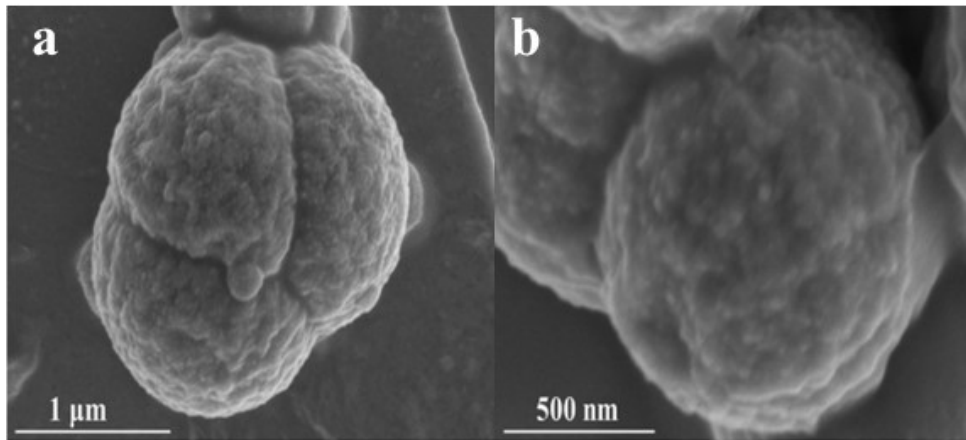
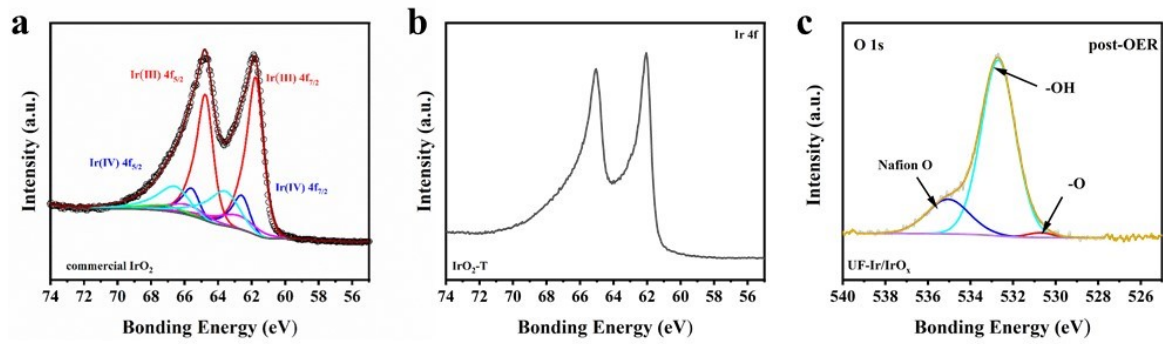
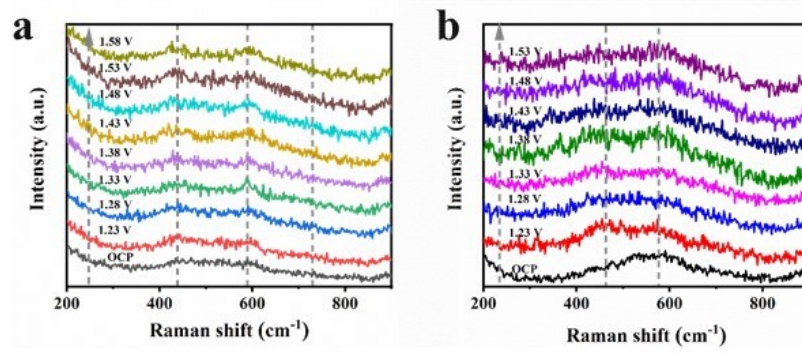


Fig. S1 SEM images of UF-Ir/IrO<sub>x</sub>.



**Fig. S2** High-resolution XPS spectra of (a) commercial IrO<sub>2</sub> and (b) IrO<sub>2</sub>-T: Ir 4f. (c) O1s of UF-Ir/IrO<sub>x</sub> after OER.



**Fig. S3** *In situ* Raman spectra of (a) IrO<sub>2</sub>-T/carbon paper and (b) commercial IrO<sub>2</sub>/carbon in 0.5 M H<sub>2</sub>SO<sub>4</sub> (with H<sub>2</sub>O).

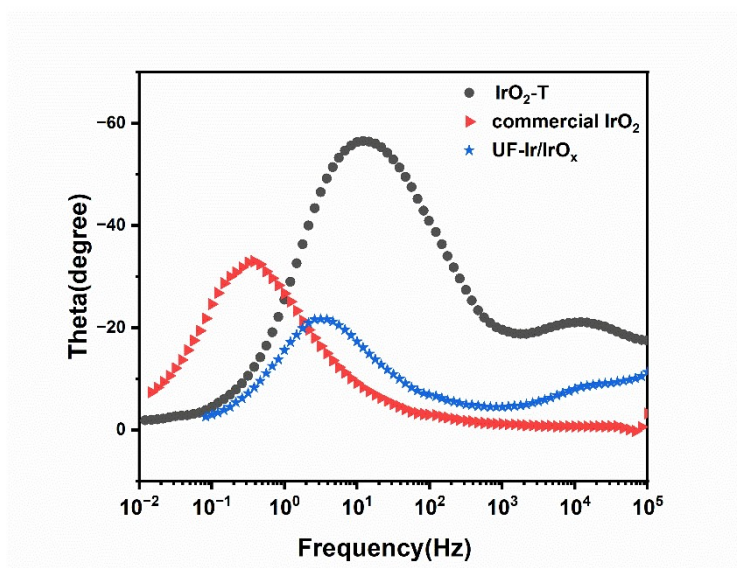


Fig. S4 Bode plots of UF-Ir/ $\text{IrO}_x$ , commercial  $\text{IrO}_2$  and  $\text{IrO}_2\text{-T}$ .

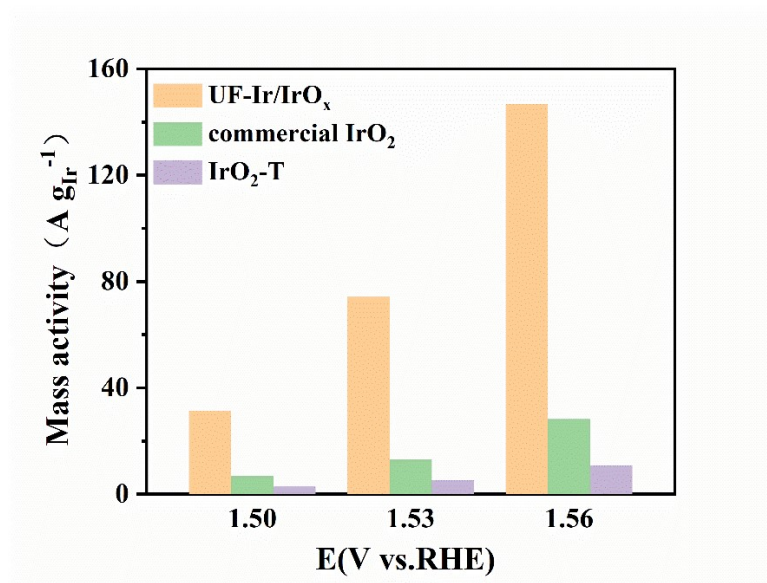
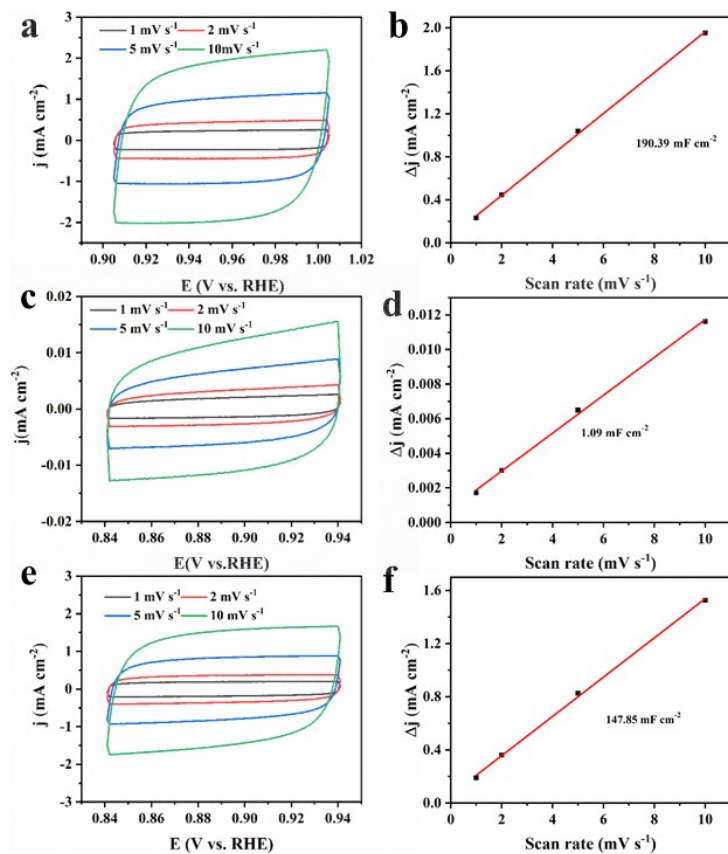


Fig. S5 Mass activity at different applied voltages of UF-Ir/IrO<sub>x</sub>, commercial IrO<sub>2</sub> and IrO<sub>2</sub>-T



**Fig. S6** (a) CV curves of UF-Ir/IrO<sub>x</sub> at different scan rates (1, 2, 5, 10 mV/s) from 0.841 to 0.941 V vs. RHE. (b) The difference ( $\Delta j$ ) between capacitive currents as a function of scan rate to give the double-layer capacitance ( $C_{dl}$ ) for UF-Ir/IrO<sub>x</sub>. For comparison, CV curves of (c) IrO<sub>2</sub>-T and (e) commercial IrO<sub>2</sub> at different scan rates (1, 2, 5, 10 mV/s) from 0.841 to 0.941 V vs. RHE are also measured, and the corresponding  $C_{dl}$  values (d, f) are also calculated.

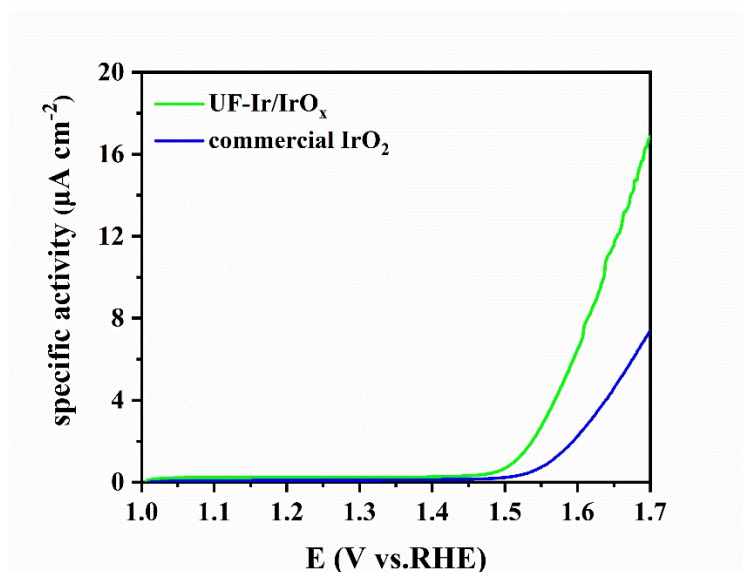
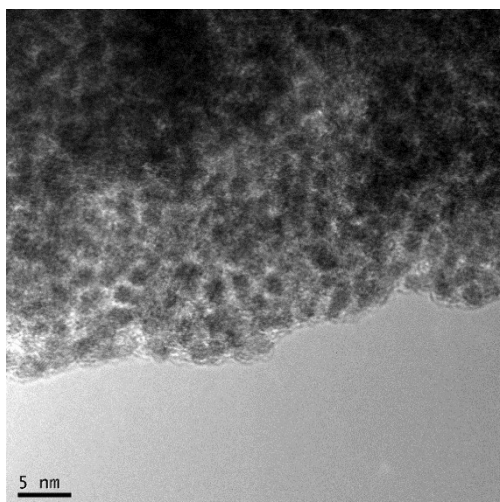


Fig. S7 ECSA-normalized LSVs for UF-Ir/IrO<sub>x</sub> and commercial IrO<sub>2</sub>.



**Fig. S8** HR-TEM image of UF-Ir/IrO<sub>x</sub> after durability test.

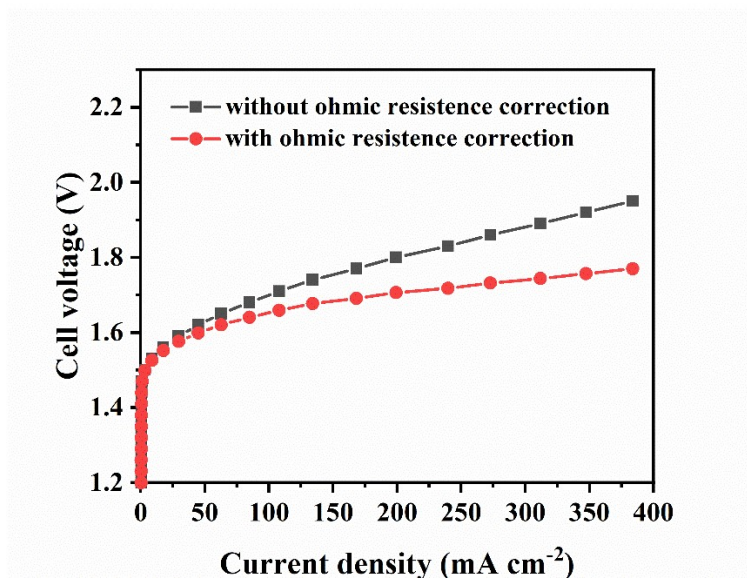
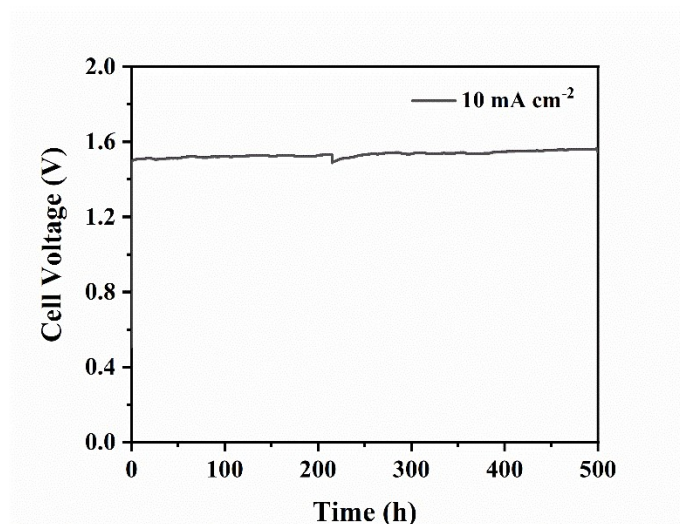


Fig. S9 Polarization curves of the PEM electrolyzers using UF-Ir/IrO<sub>x</sub> as anode and Pt/C as cathode at 25°C.



**Fig. S10** Chronopotentiometry curve of the PEM electrolyzer using UF-Ir/IrO<sub>x</sub> operated at  $10 \text{ mA cm}^{-2}$ .

**Table S1.** Content of organic elements in UF-Ir/IrO<sub>x</sub>.

<b>Elements</b>	<b>C</b>	<b>H</b>
<b>Content</b>	<b>7.19%</b>	<b>2.26%</b>

**Table S2.** The OER activity of Ir/IrO<sub>x</sub> reported in literatures.

Catalyst	$\eta@10 \text{ mA cm}^{-2}(\text{mV})$	$j_m(@=1.53 \text{ V vs. RHE})$ (A g <sub>Ir</sub> <sup>-1</sup> )	Ref
UF-Ir/IrO <sub>x</sub>	299	132	This work
IrO <sub>2</sub> NPs	370	30	J. Phys. Chem. Lett. 2012, 3, 399
IrO <sub>x</sub> /Lu <sub>2</sub> Ir <sub>2</sub> O <sub>7</sub>	301	78(@1.525 V <sub>RHE</sub> )	ACS Appl. Mater. Interfaces 2021, 13, 29654
IrO <sub>2</sub> nanospheres	352	58(@1.51 V <sub>RHE</sub> )	ACS Appl. Nano Mater. 2022, 5, 3, 4062
IrO <sub>x</sub> -Ir	-	8.1(@1.48 V <sub>RHE</sub> )	Angew. Chemie 2016, 128 (2), 752
H <sub>x</sub> IrO <sub>3</sub> nanosheet	277	120(@1.58 V <sub>RHE</sub> )	ACS Appl. Energy Mater. 2022, 5, 6, 6869
IrO <sub>2</sub> nanoneedles	313	52(@1.55 V <sub>RHE</sub> )	Adv. Funct. Mater. 2018,28(4),7
Ir atomic cluster/IrO <sub>2</sub> nanoneedles	308	62(@1.55 V <sub>RHE</sub> )	Journal of Power Sources 2022, 524, 7.
IrO <sub>2</sub> NPs/TiO <sub>2</sub>	-	59	Appl. Mater. Today 2021, 24, 15.